Numerical Prediction of Hovering Rotor Tip Vortex using Vortex Tube Model Boundary Condition

Wooyoung Choi [1], Seunghoon Lee [1], Jiyoung Jung [1], Soogab Lee [1]

[1] School of Mechanical and Aerospace Engineering, Seoul National University, Seoul, Korea
e-mail: yanni1@snu.ac.kr

Key words: Rotor, Tip vortex, Hovering, Vortex Tube, Axial Flight

Abstract

Motivated by the demand for the improved far boundary condition in the CFD computation of helicopter rotor aerodynamics, the theoretical model using vortex tube concept was applied to the far boundary condition. This model assumes that the mean rotor wake is represented by the truncated vortex tube of continuously distributed vorticity. Velocity components induced by the vortex tube are calculated at each boundary of the computational domain and applied to the far boundary condition. The aerodynamic prediction was performed about UH-60A hovering rotor based on this model and the result was compared with that of the conventional source-sink boundary condition for the effective prediction of rotor tip vortex in hovering state. The HeliNA –Helicopter Navier-Stokes equation solver- with the overset grid system was used for all the computation. The results of vortex tube model boundary condition have better accuracy for the prediction of rotor wake than that of source-sink boundary condition. In addition, the velocity components induced by the vortex tube in the whole flow fields can be used as the initial condition, instead of the initial condition of quiescent flow. It gives a good convergence characteristic for the performance prediction. The overall results show that the vortex tube model can be good alternative of the source-sink model for better numerical analysis of helicopter rotor.

1. INTRODUCTION

The prediction of the rotor wake system is the main issue in the aerodynamic design and analysis of helicopter rotor. It is important to the accurate prediction of rotor loads, performances, and acoustic. However prediction of the rotor wake is one of the most challenging problems in CFD. Over the past few years, many CFD methods have been developed for the rotor computation. One of the key problems is to reduce a numerical dissipation for the accurate prediction of rotor tip vortices. To reduce numerical dissipation, unstructured grids or overset grids have been generally used. Hariharan and Sankar [1] used high-order scheme and Usta adapted WENO[2] scheme and improved accuracy of tip vortices in hovering rotor.[3]

To specify far boundary condition is another difficult problem for the computation of hovering state. In case of hovering or descending flight, the rotor tip vortices usually do not pass away and are located very near the rotor blade. So it makes strong influence on the overall performance and causes complex flow around rotor. The most ideal condition is to adopt sufficiently large computational domain without allowing inflow or outflow at the boundaries. If we assume the quiescent flow outside of computational box, then the flow into and out of the box will be zero. This creates a closed box environment for the rotor, and the flow inside the box is recirculating when the rotor is spinning. In principle, this is precisely the environment in many hover test chambers[4]. However such a large computational box

of this size requires much computation time and cost. If a smaller computation box is adopted for the computational cost and efficiency, a non-zero flow far boundary should be specified, which allow inflow and outflow at the boundaries without violating the mass conservation law.

Most of the previous hovering rotor calculations used the far boundary conditions with the approximate source-sink model[4]. This model is based on the simple momentum theory. It assumes that a point sink is placed at the center of rotor hub to specify the inflow into the computational domain. Many previous researches have shown that the source-sink model has a good convergence characteristic and predicted the overall performance well. However, it is debatable to set the inflow velocity components toward the rotor hub at all far boundaries except the outflow region below the rotor disk. Furthermore, the radius of outflow region and the strength of outflow are almost constant regardless of rotor overall thrust or grid size. Thus, previous studies show a rather poor prediction of tip vortex geometry[5]. The tip vortex generated by preceding blade passes the rotor more closely in computation than the experimental result, and its vertical descent and radial contraction are not agree with the experimental data after a half revolution. In addition, the application of source-sink model is limited to just only hovering analysis because of its assumption.

Wang[6] proposed an analytic model for the calculation of the mean induced flow through the rotor disk in axial flight. This model was based on the simplifying assumptions about the nature of the mean flow through the rotor, leading to a simple representation of the mean rotor wake by a truncated vortex tube of continuously distributed vorticity[7]. This analytic model shows good agreement with the experimental results of the time-wise mean induce velocity averaged over the rotor disk area, for a wide range of descent rates, including vortex ring and turbulent wake flow.

In this research, this vortex tube model is applied to the far boundary condition instead of the source-sink model. Although this analytic model is originally devised to calculate induced velocity through the rotor disk, velocity induced by vortex tube can be calculated through the whole flow field around a rotor. Therefore, it is probable that more physical boundary condition can be applied for hovering and vertical flight analysis than the conventional boundary condition.

This paper deals with the flow analysis and the aerodynamic performance prediction of the hovering case. An overset grid system and WENO scheme are used. The primary purpose of this work is to analyze the possibility of vortex tube model as a far boundary condition for the rotor analysis.

2. Numerical Method

2.1 Navier-Stokes Flow solver

The three-dimensional Reynolds-averaged Navier- Stokes equations with the Baldwin-Lomax turbulence model are used for the numerical analysis. The Roe's flux difference splitting scheme combined with the Weighted Essentially Non-Oscillatory (WENO) [2] approach is applied for the higher-order spatial accuracy, and the LU-SGS method is adopted to perform the temporal integration. In case of hovering rotor, there are some useful characteristic to reduce computational burden. Its flow field is steady state when it is observed from a blade-fixed coordinate. So the source term formulation from Chen et al [8] is implemented to governing equation instead of moving rotor grid.

$$\frac{\partial \vec{q}}{\partial \tau}+\frac{\partial \vec{\hat{F}}_I}{\partial \xi}+\frac{\partial \vec{\hat{G}}_I}{\partial \eta}+\frac{\partial \vec{\hat{H}}_I}{\partial \zeta}=\frac{\partial \vec{\hat{F}}_V}{\partial \xi}+\frac{\partial \vec{\hat{G}}_V}{\partial \eta}+\frac{\partial \vec{\hat{H}}_V}{\partial \zeta}+R \tag{1}$$

Here, source term R is expressed as:

$$R=J^{-1}\begin{pmatrix}0\\ \Omega\rho v\\ -\Omega\rho u\\ 0\\ 0\end{pmatrix} \tag{2}$$

Where, Ω = angular velocity of rotor
Secondly, entire flow field goes through periodicity. And all the test cases in this work are 4 blade cases, so the size of computational domain is reduced by the factor 4 by using periodicity in hovering case.

2.2 Source-Sink Boundary Condition

Most of the hovering computation use the source-sink boundary condition to prescribe the outflow of rotor wake, which is proposed by Srinivasan[4] in 1993
The model is based on the momentum theory and the outflow velocity is defined as follow

$$W_{out}=-2M_{tip}\sqrt{C_T/2} \tag{3}$$

The radius of this outflow boundary is set by $1.12R/\sqrt{2}$ empirically. On the contrary, the inflow is assumed by a point sink of mass which is located at the center of rotor hub. Its strength is determined to satisfy mass conservation across the boundaries of computational domain. Inflow velocity is set to W_{in} and its direction is toward the rotor hub at all the boundaries.

$$W_{in}=-\frac{M_{tip}}{4}\sqrt{\frac{C_T}{2}}\left(\frac{R}{d}\right)^2 \tag{4}$$

Where, $d^2=x^2+y^2+z^2$

2.3 Vortex Tube Model Boundary Condition

Vortex tube model[6] was devised to calculate the induced velocity through the rotor disk in axial flight. Vortex tube model is as a first step beyond the disk momentum theory incorporating some sense of the rotor wake as a vertical system[7]. By applying the classical vortex theory to the vortex model, a simple relation between the induced velocity and descent velocity of the helicopter rotor has been obtained in the form of a pair of parametric equations. As shown in Fig.1, this vortex tube generates a large recirculating flow, which enters into the rotor disk at the top of the vortex tube and comes out through the bottom of vortex tube. Taking a straight vortex tube as following equations, the induced flow properties may be easily calculated. Consider a rotor producing a vortex wake represented by the constant radius tube of continuous distributed vorticity aligned with the tube circumference with an axial spatial density. The flow induced by vortex tube has axial symmetry. The tube boundary

contains vorticity strength of γ per unit length. According to the Biot-Savart law, the element $\gamma d\vec{s}$ produces an induced velocity at an arbitrary observer point $\vec{p}$. Expressed in following vector form;

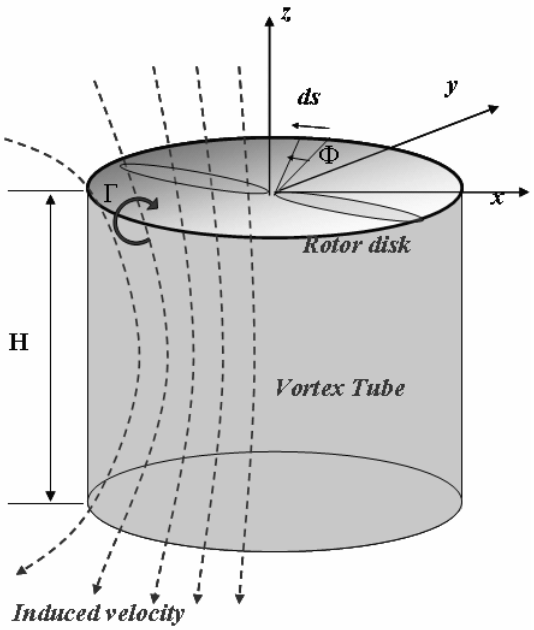

Fig.1: Vortex Tube Model schematic

$$\begin{aligned}
\vec{p} &= x_p\hat{i} + y_p\hat{j} + z_p\hat{k} \\
\vec{s} &= r\cos\phi\hat{i} + r\sin\phi\hat{j} + z\hat{k} \\
\vec{d} &= (x_p - r\cos\phi)\hat{i} - r\sin\phi\hat{j} + (z_p - z)\hat{k} \\
d\vec{s} &= -r\sin\phi d\phi\hat{i} + r\cos\phi d\phi\hat{j}
\end{aligned} \tag{5}$$

$$d\vec{v}(p) = \frac{\Delta\Gamma dz}{4\pi}\frac{d\vec{s}\times\vec{d}}{d^3} \tag{6}$$

Vortex strength γ is calculated from the thrust coefficient. After the equation is integrated along azimuthal and axial directions for the entire vortex tube, an induced radial velocity and an axial velocity at an arbitrary point $\vec{p}$ are expressed in following equations.

$$\bar{v}_r(p) = -\int_0^{\bar{H}}\int_0^{2\pi}\frac{1}{2\pi\bar{V}_t}\frac{\left(1-\frac{\bar{z}}{\bar{H}}\right)\left[(\bar{z}_p-\bar{z})\cos\phi\right]}{\left[\bar{x}_p^2+1-2\bar{x}_p\cos\phi+(\bar{z}_p-\bar{z})^2\right]^{3/2}}d\phi d\bar{z} \tag{7}$$

$$\bar{v}_z(p) = -\int_0^{\bar{H}}\int_0^{2\pi}\frac{1}{2\pi\bar{V}_t}\frac{\left(1-\frac{\bar{z}}{\bar{H}}\right)\left[1-\bar{x}_p\cos\phi\right]}{\left[\bar{x}_p^2+1-2\bar{x}_p\cos\phi+(\bar{z}_p-\bar{z})^2\right]^{3/2}}d\phi d\bar{z} \tag{8}$$

Normalized vertical transport velocity $\bar{V}_v$ and normalized vortex tube length $\bar{H}$ are varied with the descending velocity[6].

It is possible to compute analytic solutions for the entire flow fields by using derived equation (7), (8). Thus velocity components are calculated at each far boundary. By the use of these inflow velocities, inflow/outflow boundaries can be determined. For the inflow boundary, density and pressure can be calculated using isentropic relation between the boundary fields and the stagnation flow at infinity[5]. For the outflow boundary, freestream pressure is prescribed, and all other quantities are extrapolated from the interior. The resulting mass outflow automatically is adjusted to match the inflow. Finally, all the calculated flow quantities are applied to the far field boundary.

2.4 Initial Condition using Vortex Tube Model

In general, quiescent flow around rotor is given as the initial condition for the hovering computation. Because entire flow fields are generated based on the rotor overall thrust by the vortex tube model, these flow properties can be used as an initial condition for the convergence acceleration. The initial condition derived by the vortex tube model was used and compared with the conventional initial condition.

2.5 Overset Grid

To capture tip vortices accurately, an overset grid system was used. The grid system is composed of one C-H type main rotor grid, three H-H type near fields grids to capture the tip vortex accurately, and one H-H type far fields grid (Fig. 2). Two-cell overlaps have been used between adjacent grids to improve the accuracy of the flow information exchanges in the overset grid. The C-H grid on the rotor contains 161×110×50 grids point in the chordwise, spanwise, and normal directions. The H-H grid in the near fields and the far fields contains 110×150×50 grids point in the radial direction, the normal direction and the azimuth direction. Total grid point is about 4.5 million. The solution was computed on a parallel machine.

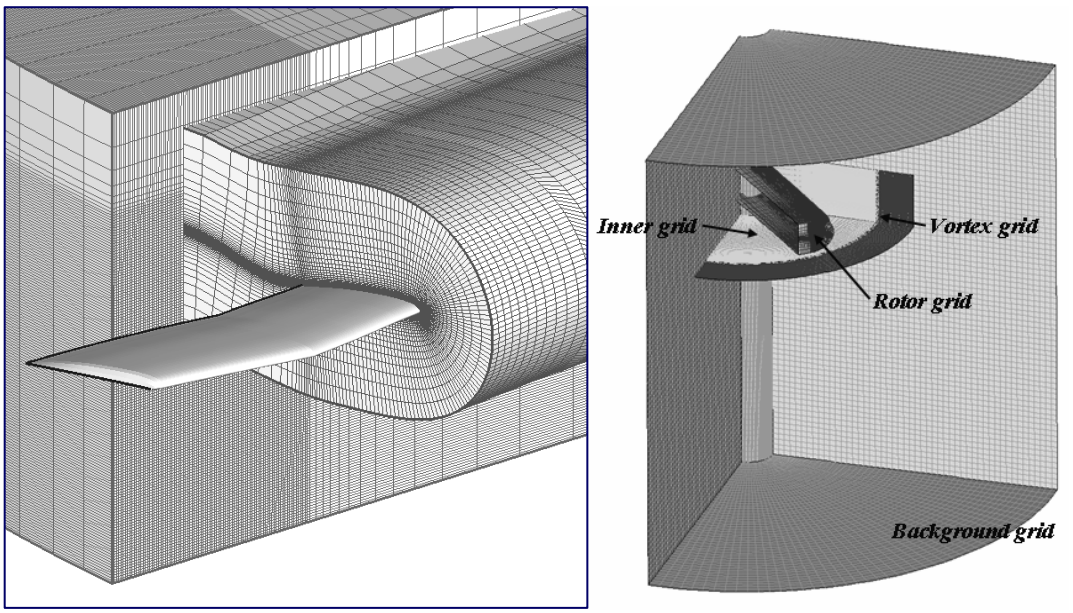

Fig.2: Overset grid schematic

3. Result and Discussion

All the test cases of UH-60A model rotor were computed for the hovering performance and the tip vortex characteristic. All cases were computed at the same tip Mach number for the validation and comparison.

3.1 Vortex Tube Model Test Case

Figure 3 presents flow field induced by a vortex tube for the hovering state of the UH-60A model. The vortex tube generated a strong downwash below the rotor disk and a recirculating flow. The strength of downwash at a bottom grid is approximately same as that of source-sink model. However, the radius of outflow region in vortex tube model is a little larger than that of outflow region in the source-sink model. These flow properties at grid boundaries were applied as the far boundary conditions in HeliNA code.

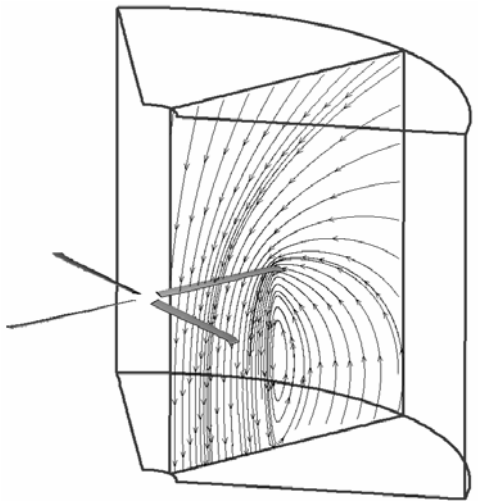

Fig.3: Flow fields induced by vortex tube model

3.2 Performance Result (UH -60A)

The hovering calculation was performed for the UH-60A model rotor[9]. The results of overall thrust and power for the test case are shown in Fig.4. The computed results of both models show good agreements with experimental result. In addition to overall rotor performance validation, Figure 5 compares the experimental and computed sectional thrust distributions. For the test case in Fig.5, note that computed results of both boundary condition shows good agreements with the experimental data. But all the computed results show CT overprediction near the rotor tip, though the result of the vortex tube model shows slightly better accuracy in the rotor tip. It is one of the chronic problems in CFD analysis of a hovering rotor. These results are deeply concerned with the smaller vertical miss distance of tip vortex beneath the rotor blade and the larger vortex core radius in computed results than those in real case[5]. As a rule, the vortex tube model seems to be successfully adopted as the far boundary condition for the hovering analysis.

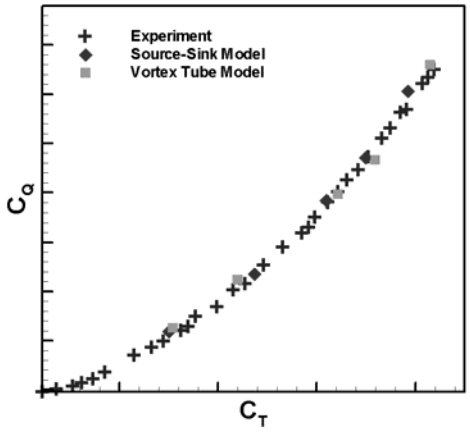

Fig.4: Thrust and power results

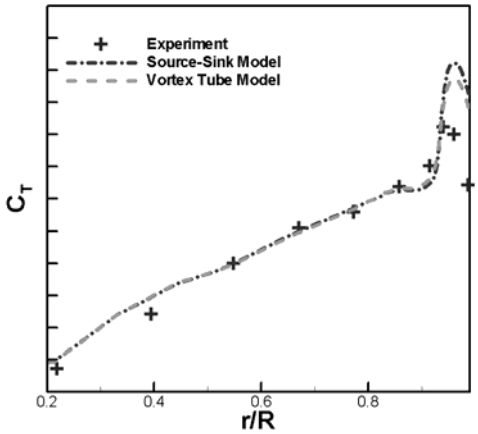

Fig.5: Sectional thrust distribution

3.3 Initial condition using Vortex Tube Model

Most of the rotor computations assume a quiescent flow field around the rotor at the start of numerical computation. As a result, the abrupt rotating of rotor blade generates much stronger tip vortex than the usual tip vortex. Thus it requires many iteration steps to eliminate this spurious rotating flow. Figure 6 shows a general C_T convergence history. Many previous hovering computations have similar convergence histories, which has the large increases of C_T at the early stage of computation, because there is no downwash through the rotor disk, which results in decrease of effective angle of attack. As iteration step goes on, rotating rotor blades generate the downwash through the rotor disk, thus the effective angle of attack is decreased, and computed thrust is also decreased to the converged thrust. It requires much time to converge thrust in the conventional initial condition. The problem is that there is no information of the flow fields at an initial stage. So there is no choice except the quiescent flow as an initial condition. However, initial condition for entire flow fields can be approximately obtained by using the vortex tube model. This initial condition using vortex tube model can remarkably accelerate the convergence, as shown in Fig.6. Because downwash induced by the vortex tube is included in the initial condition, which prevents the steep increase of the thrust at the initial stage of computation. This is the one of the important advantages of the vortex tube model for the rotor CFD analysis.

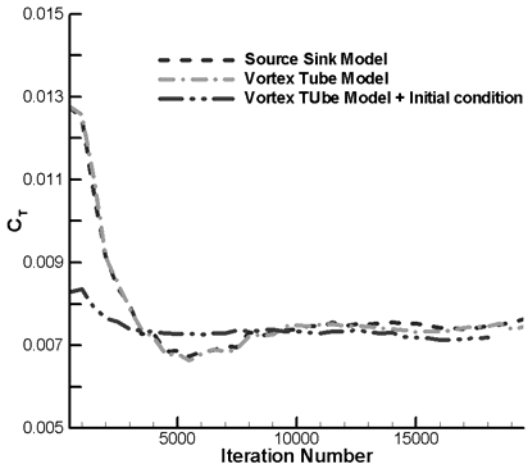

Fig.6: Thrust convergence history

3.4 Boundary Condition Effects on Rotor Wake

In Fig.7, the result using the source-sink boundary condition shows that the rotor induces a large scale rotating flow outside the rotor wake, which is usually called starting vortex. It is caused by the abrupt start of rotor rotating in numerical computation. As iteration step goes on, this rotating flow is detached from the rotor disk and finally stacked up and distorted at the bottom inflow boundary, which seems to be non-physical. The outflow region should be empirically specified inside the rotor wake region in the source sink model, but this rotating flow is moving down outside the rotor wake region as shown in Fig.7. So this spurious flow can not exit the bottom boundary, and is distorted by the downwash. It is probable that it takes negative effect on the prediction of rotor wake geometry. So it may require a rather larger grid to prevent the effect of the distorted flow. Roger et al.[5] showed that C_T and C_Q values show little change beyond 3R boundary location. In this research, the far boundaries are located 1.2 blade radii from the rotor tip in all direction. It is observed that the overall rotor performances are hardly changed regardless of the far boundary condition or far field grid size. However, tip vortices seem to be sensitive to the far boundary condition, in case that far boundary is relatively small.

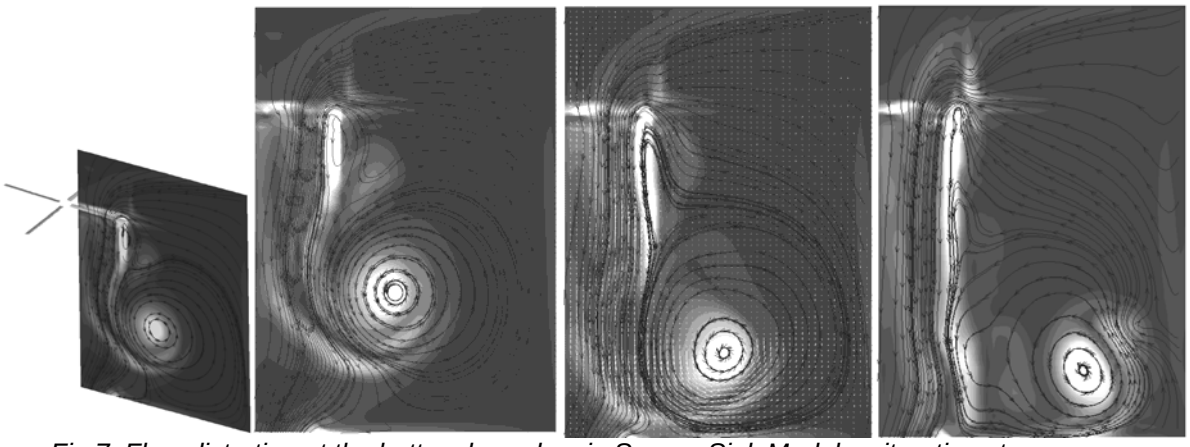

Fig.7: Flow distortion at the bottom boundary in Source-Sink Model as iteration step goes on

In contrast to the source sink boundary condition, the vortex tube model boundary condition is free from the flow distortion in bottom boundary. The differences of rotor wake in both boundary conditions are shown in Fig.8. The result of the vortex tube model boundary condition shows more stable wake structure, while rotor wake was distorted and quickly dissipated before 1 revolution in the source-sink model. Far boundaries should be located far from the rotor hub to reduce the influence of this distorted flow. It is possible to adopt smaller grid by using the vortex tube model, because all the flow properties at the boundary are extracted from the entire flow fields which are computed by the vortex tube model.

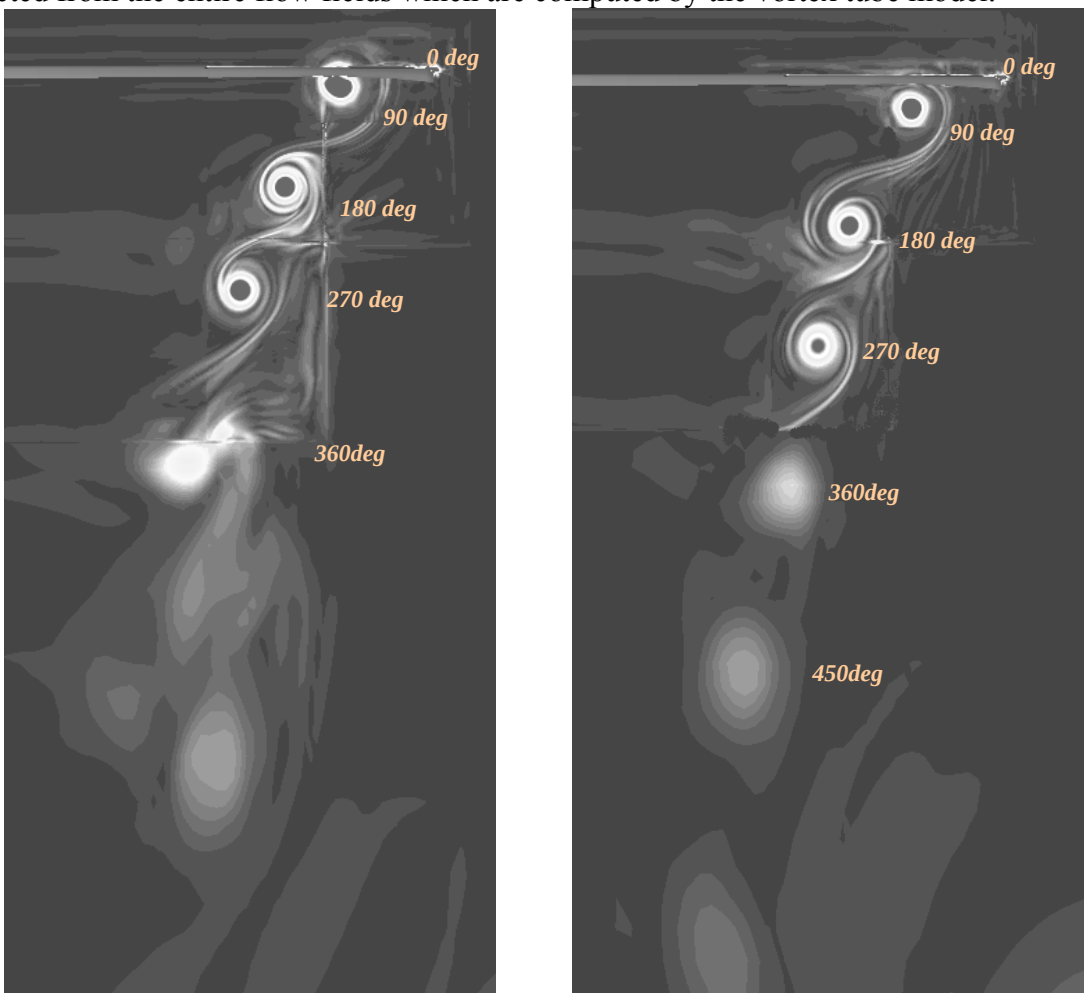

a) Source-Sink Model *b) Vortex Tube Model*

Fig.8 Computed vorticity contour on a cutting plane located 0 deg behind the rotor blade

Another difference between two boundary conditions is vertical miss distance at 90 deg wake age. Figure 8 shows that the computed tip vortex passes under the rotor blade by 0.2c in the source sink model and 0.36c in the vortex tube model, while the miss distance is about 0.4c in the experimental result. It is certain that vortex tube model boundary has better accuracy than source sink model. In spite of relatively small difference of miss distance between the experimental result and vortex tube model result, the sectional thrust was consistently overpredicted at the rotor tip as shown in Fig.5. It may results from the larger vortex core radius in the computation than in experiment.

Lorber et al.[9] presented experimental measurements for the geometry of rotor tip vortices. Fig. 9 shows vertical tip-vortex descent and Fig. 10 shows tip vortex radial contraction for a moderate thrust condition. Computed rotor wake geometry using the vortex tube model boundary condition has better accuracy in the prediction of rotor wake than the source sink boundary condition. Three dimensional rotor wake structure can be clearly seen in Figure 11, which is the iso-vorticity contour of vortex tube model case.

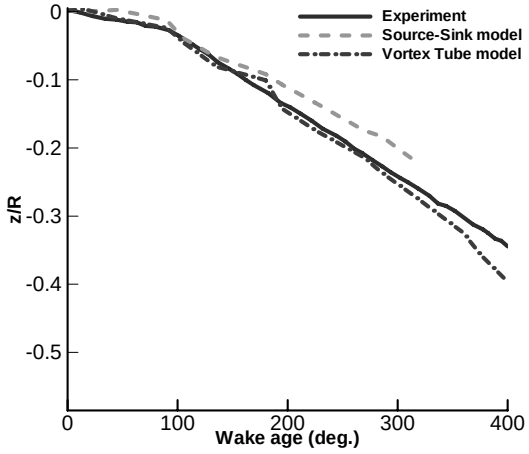

Fig.9 Tip-vortex vertical descent

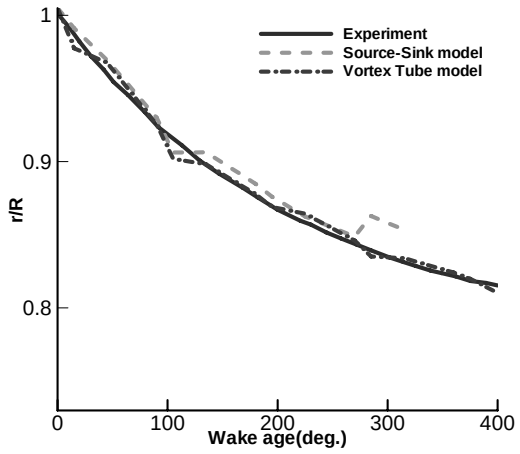

Fig.10 Tip-vortex radial contraction

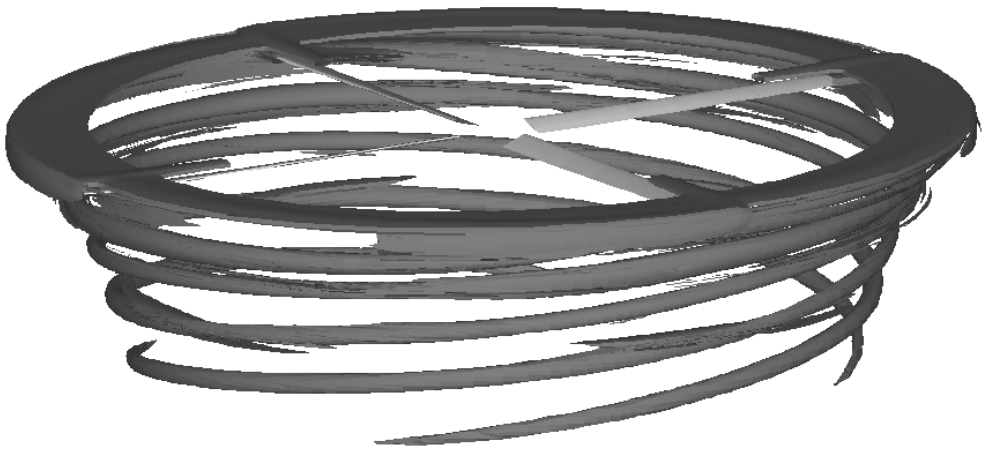

Fig.11 Iso-vorticity(0.2) surfaces of the tip (Vortex Tube Model)

4. Conclusion

This research has been designed to investigate a new boundary condition for the helicopter rotor analysis. Conventional source-sink model has weakness in the prediction of wake capturing, and a limited application-hovering only. To settle this problem, the vortex tube model is applied to the far boundary condition instead of the source-sink model. This analytic model shows good agreements with the experimental performance data and better accuracy in

the prediction of rotor wake. In addition, it is possible to reduce computational time for a convergence by adopting entire flow fields induced by vortex tube as an initial condition without losing the accuracy of the performance prediction. The overall results indicate that the vortex tube model can be a good alternative of the source-sink model for better numerical analysis of helicopter rotor.

Acknowledgements

This work is outcome of the fostering project of the Best Lab supported financially by the Ministry of Commerce, Industry and Energy (MOCIE) in Korea.

References

[1] Hariharan, N., and Sankar, L. N., "Application of ENO Schemes to Rotary Wing Problems", AIAA Paper 95-1892, June 1995

[2] Jiang, G., and Shu, C.-W., Efficient Implementation of Weighted ENO Schemes, Journal of Computational Physics, v126 (1996), pp.202-228.

[3] Usta, E.,Wake,B. E., Egolf, T.A.,Sankar, L.N., "Application of A Symmetric Total Variation Diminishing Scheme To Aerodynamics and Aeroacoustics of Rotors", American Helicopter Society 57th Annual Forum, Washington DC, May 9-11, 2001

[4] Srinivasan, G. R., Raghavan,V., Duque, E. P. N., and McCroskey,W.J., "Flow field Analysis of Modern Helicopter Rotors in Hover by Navier–Stokes Method", Journal of the American Helicopter Society, Vol. 38, No. 3, 1993, pp. 1–11

[5] Roger C. Strawn, M. Jahed Djomehri, "Computational Modeling of Hovering Rotor and Wake Aerodynamics", Journal of Aircraft, Vol. 39, No. 5, September–October 2002

[6] Wang Shi-cun, "Analytical Approach to the Induced Flow of a Helicopter Rotor In Vertical Descent" , J AHS, Vol 36, Issue 2, Jan 1990, pp92-98.

[7] Ian Simons, Wayland YF Chan, F John Perry, Richard E Brown, Gary A Ahlin, "Modelling the Mean Through a Rotor in Axial Flight Including Vortex Ring Condition", The 2nd International Basic Research Conference on Rotorcraft Technology, Nanjing, China, Nov. 7-9, 2005, pp. 98–126

[8] Chen, C. L., McCroskey, W. J., and Obayashi, S., "Numerical Solutions of Forward-Flight Rotor Flows Using an Upwind Method, Journal of Aircraft", Vol. 28, No. 6, 1991, pp. 374–380.

[9] Lorber, P. F., Stauter, R. C., Landgrebe, A. J., "A Comprehensive Hover Test of the Airloads and Airflow of an Extensively Instrumented Model Helicopter Rotor", Proceedings of the 45th Annual Forum, American Helicopter Society, May 1989, pp. 281–295